PRE-TRAINED VISION-LANGUAGE MODEL SELECTION AND REUSE FOR DOWNSTREAM TASKS

Anonymous authors
Paper under double-blind review

ABSTRACT

Pre-trained Vision-Language Models (VLMs) are becoming increasingly popular across various visual tasks, and several open-sourced VLM variants have been released. However, selecting the best-performing pre-trained VLM for a specific downstream task is challenging since no single VLM can achieve promising performance on all downstream tasks, and evaluating all available VLMs is impossible due to time and data limitations. To address this problem, this paper proposes a novel paradigm to select and reuse VLM for downstream tasks, called Model Label Learning (MLL). The proposal contains three key modules: *model labeling*, which assigns labels to each VLM to describe their specialty and utility; *model selection*, which matches the requirements of the target task with model labels; and *model reuse*, which applies selected VLMs to the target task in an ensemble manner. The proposal is highly computationally efficient and growable since the model labeling process is completed target task independent and the ability could grow with the number of candidate VLMs. We also introduce a new benchmark for evaluating VLM selection methods, including 49 VLMs and 17 target task datasets. Experimental results clearly demonstrate the effectiveness of the proposed method for selecting and reusing VLMs.

1 INTRODUCTION

Vision-Language Models (VLMs), such as CLIP (Radford et al., 2021), ALIGN (Jia et al., 2021), etc, which are pre-trained on large-scale image-text datasets, have recently attracted significant attention due to their remarkable zero-shot prediction capabilities on visual tasks. However, though VLM shows impressive general ability, as highlighted in Radford et al. (2021), VLMs often fall short of supervised expert models in many downstream tasks. To address this limitation, numerous studies (Dosovitskiy et al., 2021; Yu et al., 2022; Fang et al., 2023) have sought to enhance the zero-shot performance of VLMs by studying model architectures, pre-training datasets, and training/fine-tuning methods. This effort has led to the development of many open-source pre-trained VLMs with diverse structures and parameters, contributing to VLM model hubs like open-clip (Ilharco et al., 2021), which currently hosts more than 100 pre-trained VLMs.

As more and more VLMs are open-sourced, the problem of how to select a VLM to reuse for specific downstream tasks naturally occurs. Although we can directly utilize the best-performing model on a universal dataset such as ImageNet, previous work (Fang et al., 2022) has shown that the performance of VLMs can vary greatly depending on dataset domain. For example, we evaluate the performance of various pre-trained VLMs in the open-clip library across several downstream tasks (1(a)) and within different classes of a specific task (1(b)). Figure 1(a) reveals that each VLM demonstrates distinct strengths in zero-shot visual tasks, with no single model outperforming all others across every task. Interestingly, models that perform worse on general tasks can sometimes surpass stronger models in specific downstream tasks. Furthermore, even in the same task, different VLMs exhibit varying levels of performance across specific classes, as illustrated in Figure 1(b).

Therefore, it is important to design VLM selection methods, and it would be better if we could achieve more fine-grained selection, i.e., select different VLMs to handle different classes. The direct way to select a model is to evaluate all candidate models' performance on the target task. However, it is unrealistic due to time and computational resource limitations. Additionally, previous works on model selection (Tran et al., 2019; You et al., 2021) primarily focus on single-modal

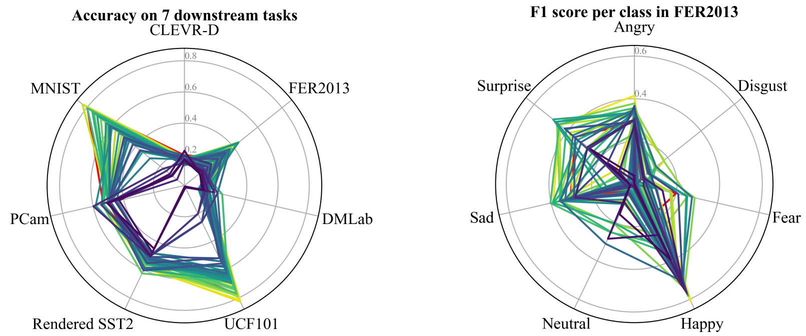

(a) Accuracy of VLMs on 7 specific downstream tasks.

(b) F1 score of VLMs per class in a downstream task FER2013.

Figure 1: The spider charts measure the models' capabilities across different downstream tasks and classes within a task, showing that the best-performing models vary across downstream tasks and classes, highlighting the importance of model selection for VLM.

models, making them unsuitable for VLM selection since they only handle either image or text output and cannot incorporate data from the other modality. Zohar et al. (2023) is the first study to focus on VLM selection, proposing to evaluate VLM performance using textual information. However, their selection strategy heavily depends on the models' ground-truth performance on large-scale datasets, such as ImageNet. When models excel on large-scale datasets but under-perform on specific tasks, selection strategy effectiveness drops, as shown later in our experiments.

To this end, we introduce a novel paradigm to select and reuse VLMs called Model Label Learning (MLL). The core idea is to organize candidate pre-trained VLMs into a model hub and describe the specialty and utility of each VLM as the model's label in some manner. When facing a new downstream task, we can match the task requirements with the model labels to select and reuse models. Specifically, the proposal contains three key interconnected modules: *model labeling*, *model selection*, and *model reuse*. In the *model labeling* process, we construct a semantic graph with commonly occurring visual concepts and representative samples, and each model undergoes pre-testing on the semantic graph to generate its model label, which describes its capability on these semantic classes. In the *model selection* process, we generate caption descriptions for both the nodes in the semantic graph and the categories to be classified in the target task to compare their similarity. This enables us to evaluate the model's performance on the target classes by aligning the matched semantic nodes with the model labels. In the *model reuse* process, we apply an ensemble strategy that combines the selected models' predictions on a single class and chooses the highest confidence across all classes as the final prediction.

The model labeling process is completed immediately when the candidate VLM is added to the model hub, therefore, it is target task independent, which means the proposal is both data and computationally efficient in the model selection process. Moreover, the proposal is highly growable since the capability could grow with the number of candidate models in the model hub and the model labels are also scalable since more semantic nodes can be added continually. Moreover, we introduce a comprehensive benchmark for evaluating VLM selection methods, aiming to facilitate related research. The benchmark includes 49 pre-trained VLMs and 17 target datasets as downstream tasks. The ground-truth model ranking for each target task is provided for evaluation. We construct a semantic graph that contains more than 9000 commonly used visual concepts to pre-test each VLM. The experiments conducted demonstrate the effectiveness of our approach in both selecting and reusing VLMs, while also validating the scalability of the model hub.

In summary, our contributions are as follows:

1. We highlight that the performance of pre-trained VLM varies across different downstream tasks and even among classes within the same task. Therefore, it is important to study the VLM selection problem which is usually neglected by related researchers.

2. We propose a novel paradigm called Model Label Learning, which encompasses the processes of model labeling, selection, and reuse. This paradigm is both time- and data-efficient, and highly scalable. It can give birth to new VLM model hubs, which can make it easier for users to select and reuse VLM to solve their tasks.
3. We introduce a new benchmark for evaluating pre-trained VLM selection and reuse methods, contributing to the advancement of research in this field. Experimental results validate the effectiveness and scalability of the proposal for selecting and reusing VLMs.

2 Related Work

2.1 Vision-Language Model

In recent years, there have been significant advances in the field of Vision-Language Models (VLMs), including notable models such as CLIP (Radford et al., 2021), ALIGN (Jia et al., 2021), BLIP (Li et al., 2022), etc. These models leverage large-scale datasets containing image-text pairs, such as WIT (Srinivasan et al., 2021), to align visual and text features within a shared embedding space, which has led to impressive capabilities in feature extraction, particularly in the realm of zero-shot visual tasks. Tremendous works (Dosovitskiy et al., 2021; Yu et al., 2022; Fang et al., 2023) attempted to improve the zero-shot capabilities of VLMs by focusing on model architecture, pre-training datasets, and training/fine-tuning methods, which lead to the emergence of numerous open-source pre-trained VLMs. As a result, several VLM model hubs are constructed, such as open-clip (Ilharco et al., 2021) and HuggingFace (Wolf et al., 2020), which provide access to numerous VLMs. However, these model hubs lack effective model selection mechanisms; users can only select models based on some quantitative indicators, such as download volume, popularity, etc.

2.2 Model Selection

As pre-trained models become increasingly diverse, how to select appropriate pre-trained models to tackle specific tasks has become a significant challenge. Many researchers have started to focus on this aspect. For example, Negative Conditional Entropy (NCE) (Tran et al., 2019) proposes an information-theoretic quantity to learn the transferability and hardness between classification tasks; LEEP (Nguyen et al., 2020) utilizes source prediction probabilities instead of hard labels compared with NCE; LogME (You et al., 2021) estimates the correlation between source model features and the target outputs by maximum evidence; MetaGL (Park et al., 2023) solves the model selection problem on graph data by introducing a meta-learning method; EMMS (Meng et al., 2023) uses weighted linear regression to estimate the transferability of candidate models; Model Spider (Zhang et al., 2024) uses a re-ranking mechanism to enhance the task-model co-embedding. Although these methods achieve well-performing in different settings, most of them focus on single-modal which cannot be directly used for VLM selection. Moreover, the training data for VLM is inaccessible, which introduces more challenges. Model selection for VLM is still a relatively new topic. LOVM (Zohar et al., 2023) uses a text dataset to describe the prediction task to train a linear model to predict the performance of the VLM. However, this method can only exploit text information and becomes less effective when there is a domain shift between the downstream tasks and the training tasks.

2.3 Learnware

Learnware (Zhou & Tan, 2022) is a novel paradigm that explores more effective model selection by constructing specifications to describe the capabilities of the model, closely aligning with our idea of model labeling. Compared with previous selection methods, learnware enables scalable and efficient model selection across diverse architectures and input types within a unified framework, improving as the system expands. Model specification is central to the learnware paradigm. Recent works (Tan et al., 2024) on learnware paradigm are built on Reduced Kernel Mean Embedding (RKME) (Wu et al., 2021), which maps training data distributions to points in Reproducing Kernel Hilbert Space (RKHS) and identifies models by comparing similarities in the RKHS. Furthermore, Guo et al. (2023) enhanced RKME for heterogeneous label spaces, while Tan et al. (2023) addressed challenges in heterogeneous feature spaces. However, learnware requires training data to construct specifications. Considering the scale of VLM pre-trained datasets, it is unrealistic to construct specifications for learnware to select models due to limited time and computational resources.

3 PRELIMINARIES

3.1 ZERO-SHOT VISION TASK OF VLM

Pre-trained VLMs for zero-shot visual tasks are built using two encoders: image encoder and text encoder. The image encoder is used to transform an image into a vector embedding, which presents its feature. The text encoder tokenizes the text input and generates a embedding representation by the text token. Let $\mathcal{I} : \mathcal{X} \rightarrow \mathbb{R}^n$ denotes the image encoder and $\mathcal{T} : \mathcal{Y} \rightarrow \mathbb{R}^n$ denotes the text encoder, where $X \in \mathcal{X}$ is the image input, $Y \in \mathcal{Y}$ is the text input, and n is the dimension of the shared multi-modal embedding space of text embeddings and image embeddings.

In a particular downstream task T, there are C_T classes $Y_T = \{y_i\}_{i=1}^{C_T}$. For a image $x \in X$, we obtain the image embeddings $\mathcal{I}(x)$ given by the image encoder $\mathcal{I}$ and the text embeddings $\mathcal{T}(y)$ of class y produced by the text encoder $\mathcal{T}$. Then, the prediction $\hat{y}$ of image x can be obtained as

$$\hat{y} = \arg\max_{y \in Y_T} \frac{\exp\left(\mathrm{sim}\left(\mathcal{I}(x), \mathcal{T}(y)\right)\right)}{\sum\limits_{y' \in Y_T} \exp\left(\mathrm{sim}\left(\mathcal{I}(x), \mathcal{T}(y')\right)\right)} \tag{1}$$

where $\mathrm{sim}\left(\cdot, \cdot\right)$ denotes cosine similarity.

3.2 PROBLEM SETUP

Assume the model hub has $\mathcal{M}$ pre-trained VLMs $\{f_m = \{\mathcal{I}_m, \mathcal{T}_m\}\}_{m=1}^{\mathcal{M}}$, where $\mathcal{I}_m$ and $\mathcal{T}_m$ denote image encoder and text encoder of the VLM f_m. There are two stages in our setting: the *submission stage* for developers to upload models and the *identification stage* for users to select models.

In the submission stage, the model developer submits a VLM f_m to the model hub, and the model hub assigns a label S_m to the model to describe its specialty and utility. It is particularly emphasized that uploaded models are anonymous, meaning we do not have access to their training data.

In the identification stage, the user attempts to select VLMs from the model hub for the zero-shot downstream task T, by uploading general information about the task, such as classes, domain type, and task type, to describe their requirements. We subsequently utilize this information to select and reuse suitable VLMs, based on the model labels established in the submission stage.

The two main problems in our settings are: 1) In the submission stage, how can we design a label to that fully characterize the capabilities of the submitted VLM? 2) In the identification stage, how can we select and reuse appropriate VLMs from the model hub to address users' downstream tasks based on their requirements and the model labels?

4 OUR APPROACH

4.1 FRAMEWORK

As illustrated in Figure 2, the MLL paradigm consists of three key modules: *model labeling*, *model selection*, and *model reuse*. In the *model labeling* process, MLL constructs a semantic graph $\mathcal{G}$ with commonly occurring visual concepts and representative samples as the evaluation datasets. When models are submitted to the model hub, they are pre-tested on the semantic graph and assigned labels S_m, which describe their capability on these semantic classes. In the *model selection* process, we generate caption descriptions for both the nodes in the semantic graph and the categories in the target task to compare their similarity. This enables us to evaluate the model's performance on the target classes by aligning the matched semantic nodes with the model labels. In the *model reuse* process, we apply an ensemble strategy that combines the selected models' predictions on a single class and chooses the highest confidence across all classes as the final prediction.

4.2 MODEL LABELING

To thoroughly characterize the capabilities of the model, we initiate the process by constructing a Semantic Graph $\mathcal{G}$ as evaluation datasets utilizing the WordNet (Miller, 1995) synsets. Firstly, we represent each synset in WordNet as a corresponding node v within the semantic graph and establish

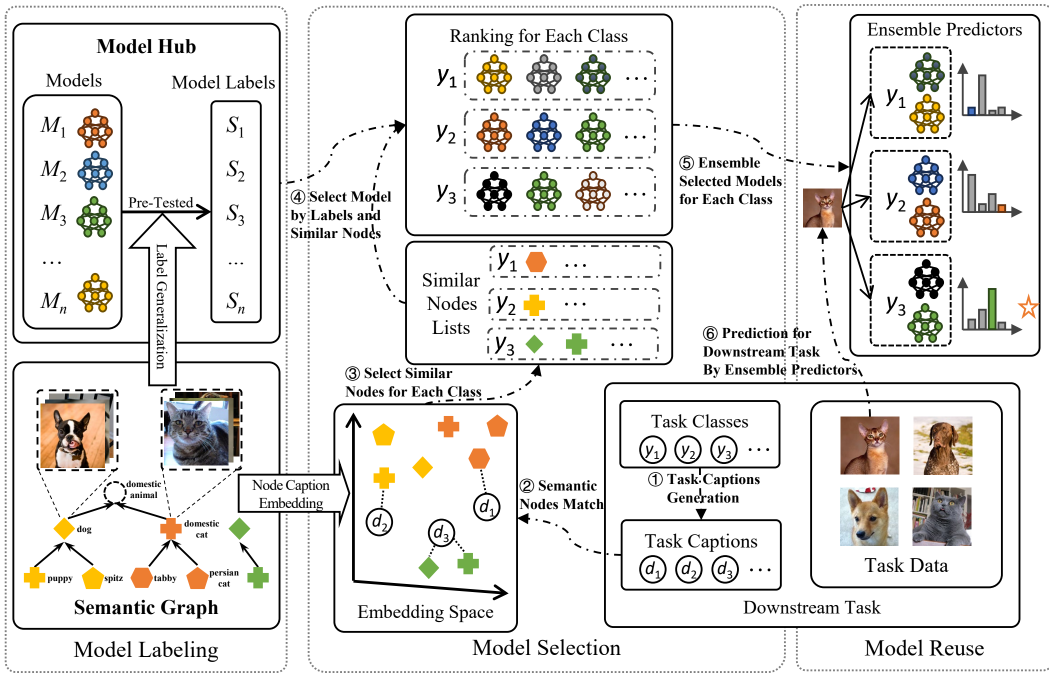

Figure 2: The framework of MLL paradigm. Models added to the hub first undergo a pre-testing phase, during which they are assigned labels that describe their specific functionalities in the labeling module. When a downstream task is presented, the system selects relevant models in the selection module and ensembles them to address the task.

links between nodes based on their relationships of hypernyms and hyponyms. Subsequently, to capture the real-world image distribution associated with each node, we randomly select images X_v from sample datasets (detailed in Section 5.1) to serve as representations for each node v. Due to the limited information in synset name, we also need obtain the caption dataset $D_{\mathcal{G}} = \{d_v | v \in V_{\mathcal{G}}\}$ for label generalization where $V_{\mathcal{G}}$ denotes the set of nodes in Semantic Graph $\mathcal{G}$, d_v denotes the caption of node v. We use "{synset name} which is {synset definition}" as the caption for each node, where "{synset name}" and "{synset definition}" correspond to the synset name and definition of a synset. Utilizing the constructed semantic graph, we generate a label S_m for each VLM f_m in the model hub that accurately reflects its capabilities.

$$s^v_{m,x} = \text{sim}(\mathcal{I}_m(x), \mathcal{T}_m(D_{\mathcal{G}})), x \in X_v \quad (2)$$

$$s^v_m = \{s^v_{m,x} | \; \forall x \in X_v\} \quad (3)$$

$$S_m = \{s^v_m | \; v \in V_{\mathcal{G}}\} \quad (4)$$

where $\mathcal{I}_m(\cdot)$, $\mathcal{T}_m(\cdot)$ denotes the image encoder and text encoder of model f_m .

Specifically, the constructed semantic graph allows for the seamless addition of new nodes and the incremental updating of model labels based on existing foundations. As the nodes in the semantic graph are expanded, its ability to reflect the performance capabilities of the models is enhanced. Once we have obtained labels for each model, we can utilize them for effective model selection.

4.3 Model Selection

In the model selection module, given a downstream task T with C_T classes $Y_T = \{y_i\}_{i=1}^{C_T}$, in order to utilize the obtained model labels S_m, we need to match the downstream task classes Y_T with the semantic graph nodes $V_{\mathcal{G}}$. However, it can not match well using original class names. Inspired by previous work (Zohar et al., 2023), we construct expanded captions for both the downstream task classes and the semantic graph nodes. Large Language Models (OpenAI, 2023) have made

Algorithm 1 Model Selection & Reuse

Input: Model hub $\mathcal{M}$, model labels $\{S_m\}$, semantic graph $\mathcal{G}$, semantic graph caption dataset $D_{\mathcal{G}}$, count k of reused models pre-class, target task $T = (X, Y)$

Output: Task prediction $\{\hat{y}\}$

1: Construct caption dataset D_T for target task T.
2: Match similar nodes V^{Selected} in $V_{\mathcal{G}}$ with Y by captions $D_{\mathcal{G}}$ and D_T.
3: Construct transfer matrix $Z \in \mathbb{R}^{V^{\text{Selected}} \times C^T}$ based on caption similarity of V^{Selected} and Y.
4: **for** $f_m \in \mathcal{F}_{\mathcal{M}}$ **do**
5: Calculate reusable metric $r_{m,y}$ for each class y in Y by Eq.$(5, 6, 7)$.
6: **end for**
7: **for** $y \in Y$ **do**
8: Select k models to ensemble predictor $\mathcal{F}_y^k = \left\{ f_m \mid f_m \in \text{top-}k \left(\{r_{m,y}\}_{\mathcal{M}} \right) \right\}$.
9: Calculate prediction $\hat{y}$ for x by Eq.$(8, 9, 10)$.
10: **end for**
11: **return** Task prediction $\{\hat{y}\}$;

significant advancements, facilitating the generation of text data. Assuming general information about the downstream tasks, such as task types and target domain, is accessible, we use GPT-3.5 with specific prompts to generate descriptions for each class as shown below, creating the caption dataset D_T for downstream task T. The following is an example of a prompt used to generate a caption of the class *cat*.

> Generate long detailed caption for the *natural picture* of *cat* in the
>
> *image classification*. e.g., " The *natural picture* of *cat*, which is ... ".
>
> Generate long caption for *cat* within *50* words.

where *natural picture* and *image classification* can be replaced with the domain and task descriptions, while *cat* can be substituted with the specific class name for the target task.

Then, we can use a language model to generate embeddings of graph captions $D_{\mathcal{G}}$ and target task captions D_T. By comparing the cosine similarity between the embeddings, we can select the top k nodes for each class based on similarity and construct a transfer matrix $Z = (z_{vy}) \in \mathbb{R}^{|V^{\text{Selected}}| \times |Y^T}$, where V^{Selected} represents all selected nodes. Additionally, z_{vy} represents the similarity of captions between graph node v and task class y if v is among the top k nodes that exhibit the highest similarity with task class y. Otherwise, it will be set to 0. Subsequently, the precision $p_{m,v}$ for each model f_m at the graph nodes v is defined as follows.

$$p_{m,v} = \frac{1}{|X_v|} \sum_{x \in X_v} \mathbb{I} \left(v = \underset{v \in V^{\text{Selected}}}{\arg\max}\; s_{m,x}^v \right) \tag{5}$$

By utilizing the transfer matrix Z, the precision prediction $p_{m,y}$ for each class y in the downstream task T can be further derived.

$$p_{m,y} = \sum_{v \in V^{\text{Selected}}} p_{m,v} \cdot z_{vy} \tag{6}$$

When a model excels in a specific class, it may incorrectly handle data not belonging to that class. Consequently, we need to select models that perform well on specific classes while also maintaining good overall performance. Thus, we introduce a weight parameter α to balance class performance with overall performance. Then, the reuse metric r for model f_m in class y is defined as:

$$r_{m,y} = \alpha \cdot p_{m,y} + \frac{1 - \alpha}{|Y_T|} \sum_{y' \in Y_T} p_{m,y'} \tag{7}$$

4.4 Model Reuse

To better utilize the selection and harness the capabilities of models in the model hub, we introduce a specific count k of models to reuse for each class y, we select up to k highest-score model to form the ensemble predictor $\mathcal{F}_y^k = \left\{ f_m \mid f_m \in \text{top-}k\left(\{r_{m,y}\}_{\mathcal{M}}\right)\right\}$. During testing, for the data $x \in X$ of the downstream task, ensemble predictor $\mathcal{F}_y^k$ infers the confidence $p_y^k(x)$ of class y:

$$p_y^k(x) = \sum_{f_m \in \mathcal{F}_y^k} w_{m,y} \cdot \frac{\exp\left(\text{sim}\left(\mathcal{I}_m(x), \mathcal{T}_m(y)\right)\right)}{\sum_{y' \in Y_T} \exp\left(\text{sim}\left(\mathcal{I}_m(x), \mathcal{T}_m(y')\right)\right)} \tag{8}$$

where $w_{m,y}$ denotes the ensemble weight obtained from the output probability entropy $\mathcal{H}$ of each model within $\mathcal{F}_y^k$, aimed at reducing the impact of unreliable predictions. $w_{m,y}$ is defined as:

$$w_{m,y} = \frac{\mathcal{H}\left(\{\text{sim}(\mathcal{I}_m(x), \mathcal{T}_m(y) | \ \forall\ y \in Y_T\}\right)}{\sum_{f_{m'} \in \mathcal{F}_y^k} \mathcal{H}\left(\{\text{sim}(\mathcal{I}_{m'}(x), \mathcal{T}_{m'}(y) | \ \forall\ y \in Y_T\}\right)} \tag{9}$$

Then, the class with the highest confidence is selected as the prediction $\hat{y}$ for x:

$$\hat{y}(x) = \arg\max_{y \in Y_T} p_y^k(x) \tag{10}$$

Flow of model selection and reuse of MLL Paradigm are summarized in Algorithm 1.

Our proposal achieves higher accuracy, efficiency, and scalability. In terms of accuracy, the proposal elucidates the functionalities of VLMs by labeling models with a semantic graph that covers the most common visual concepts and representative samples to describe different data distributions, enabling more accurate identification of suitable models for users' target tasks. For efficiency, the proposal generates model labels when the pre-trained model is uploaded to the model hub, thus, it is highly efficient in the model selection process, without the need to run the candidate models on the target dataset. Regarding scalability, the concepts in the semantic graph can be continually added, thus, the model labels are scalable flexibility. Moreover, as the number of VLMs in the model hub increases, our proposal identifies higher-quality models, leading to improved performance on zero-shot downstream visual tasks.

5 Experiments

5.1 MLL Benchmark

To evaluate the capabilities of the MLL paradigm in zero-shot visual tasks with VLMs, we need to obtain a set of sampling datasets for constructing semantic graph $\mathcal{G}$, along with another set dedicated to downstream target tasks. For this study, we select 49 VLMs, 5 Sample Datasets, and 17 Target Datasets. Additionally, we collect general information about the task types and domains associated with each dataset to provide a task description. For testing the selected models on the target tasks, we utilized the same prompting strategy outlined in Radford et al. (2021)'s work, ensuring consistency in our evaluation methodology, available at the anonymous link.

Model Hub. We leverage the open-clip library (Ilharco et al., 2021), which encompasses a diverse set of pre-trained VLMs across multiple architectural frameworks, such as ViT(Dosovitskiy et al., 2021) and ConvNet(Liu et al., 2022). These models have been pre-trained on a variety of large-scale datasets, such as WIT (Srinivasan et al., 2021) and LAION-2B (Schuhmann et al., 2022). We select 49 models from this library to form our model hub for the purpose of our experiments. All models used in the experiments are directed downloaded from the library.

Datasets. We utilized 5 datasets, ImageNet (Deng et al., 2009), ImageNet-V2 (Recht et al., 2019), ImageNet-Sketch (Wang et al., 2019), ImageNet-A (Hendrycks et al., 2021b) and ImageNet-R (Hendrycks et al., 2021a), as Sample Datasets for semantic graph construction. Additionally, we used 17 commonly used datasets and their task general information as Target Datasets to evaluate VLM selection and reuse methods in zero-shot visual tasks (as shown in Table 3). These datasets demonstrate diversity in terms of domain, number of classes, and task types. They encompass various domains, including animals, food, text, landscapes, remote sensing, medical applications, and transportation. Additionally, they cover a range of tasks such as image classification, geo-localization, optical character recognition, facial expression recognition, and object distance estimation. To eliminate interference from additional modules or training during evaluation, all tasks can be assessed using the same VLM architecture.

Table 1: Comparison of the zero-shot performance on 17 target task datasets. The best performance is highlighted in bold.

Methods	CIFAR100	Country211	CLEVR-D	DTD	DMLab	Flowers102
INB	0.8599	0.3121	0.1262	0.6787	0.1940	0.8761
ModelGPT	0.8599	0.3121	0.1262	0.6787	0.1940	0.8761
Proposal (k=1)	0.8773	0.3159	**0.1361**	0.6910	**0.2111**	**0.8914**
Proposal (k=3)	**0.8923**	**0.3238**	0.1171	**0.7053**	0.1573	0.8720

Methods	MNIST	OxfordPet	PCam	FER2013	Food101	GTSRB
INB	0.7956	0.9401	0.5332	0.2859	0.9553	0.5391
ModelGPT	0.5648	0.9401	0.4990	0.4014	0.9553	0.5391
Proposal (k=1)	**0.8210**	**0.9488**	**0.5334**	0.3904	**0.9576**	**0.5752**
Proposal (k=3)	0.8101	0.9428	0.5003	**0.4933**	0.9566	0.5636

Methods	RESISC45	Rendered SST2	StanfordCars	STL10	UCF101	Avg.
INB	0.6139	0.5199	0.9487	**0.9889**	0.7702	0.6434
ModelGPT	0.6139	**0.5800**	0.9487	0.9639	0.7702	0.6367
Proposal (k=1)	0.6437	0.5206	**0.9568**	0.9878	0.7961	0.6620
Proposal (k=3)	**0.6800**	0.5233	0.9541	0.9854	**0.8092**	**0.6664**

Evaluation Metrics. In our benchmark, methods are expected to select models from a hub of 49 pre-trained VLMs and reuse them across 17 target datasets as downstream tasks to achieve better performance. Notably, all models selected for use are without additional fine-tuning, as all downstream tasks are zero-shot. We use $Acc.$ to evaluate methods' performance on both downstream target tasks and the average performance across all tasks.

5.2 Experiment Setup

Semantic Graph Construction. We construct a semantic graph $\mathcal{G}$ containing 9055 nodes using the WordNet synsets, which contains a wide range of items, such as animals, tools, clothing, vehicles, plants, and more. Each node is represented by up to 75 randomly selected images from the sample datasets, reflecting the distribution of the node's concepts. We use OpenAI text-embedding-3-large model to obtain caption embeddings of semantic graph nodes and downstream task class nodes, we then match the similar node between them by cosine similarity between the embeddings.

Compared Methods. Initially, we compare our proposal with ImageNet Baseline (INB), which employs the performance of VLMs on the ImageNet to select which model to reuse. Additionally, we compare it with a VLM selection method called ModelGPT (Zohar et al., 2023). ModelGPT employs generated captions and synonyms for target task classes as substitutes for images of those classes, then evaluates the performance of VLMs by measuring their ability to correctly classify the captions and synonyms into their corresponding classes, which serves as the reuse metric in combination with INB. A linear model is then learned between the reuse metric and ground-truth performance on training downstream tasks. Finally, the zero-shot ability of VLMs on the target task is predicted using this linear model and the reuse metric.

Implementation Details. We adopt the official code to implement ModelGPT. For a fair comparison, the experiment utilizes the ground-truth performance of VLMs on Sample Datasets for ModelGPT to train its linear model, and then evaluate it on the benchmark. For both INB and ModelGPT, the experiment selects the model with the highest predictive performance given by the method for reuse in the target task. Specifically, we employ the same prompting strategy outlined in the work of Radford et al. (2021), which uses the prompt "a photo of {class}", where "{class}" is replaced by the task class. All selected models are utilized without any further fine-tuning, given that all downstream tasks are conducted in a zero-shot manner. Additionally, the weight α for model selection in our setting is set to 0.7. All experiments are conducted on NVIDIA A800 GPUs.

5.3 Experiment Results

Zero-shot Performance In our experimental setup, the goal is to optimize the performance of VLMs on downstream zero-shot visual tasks. Therefore, in Table 1, we compare the performance of different model selection methods across 17 benchmark datasets. We set two values for the count k of reused models, specifically 1 and 3, to test the effects of using a single model versus an ensemble of three models per class. The results show that our method achieves high performance on most downstream tasks. **ModelGPT largely aligns with INB, indicating a strong correlation in their selection strategies. When INB fails to select a well-performing model, ModelGPT also struggles with selection**. By comparing different counts k of reused models, MLL demonstrates that reusing the model with the best performance per class is often sufficient to outperform baseline methods in most downstream tasks, highlighting the practicality of the MLL paradigm. We also find that in datasets with a limited number of classes, such as PCam and MNIST, employing a single model for each class tends to yield better results. Additionally, when the models available in the model hub are generally weak, as seen in several datasets, such as CLEVR-D and DMLab, relying on ensemble methods may introduce more noise than benefit. In these cases, a single model per class often provides the ultimate balance between simplicity and effectiveness.

Scalability of Model Hub We design a scenario where the model hub starts from scratch and gradually expands until it contains all available VLMs. Figure 3 provides a detailed illustration of the average performance of 17 downstream tasks throughout 30 randomly generated expansion schemes. The results clearly show that as the model hub grows and expands, our method can more efficiently reuse the well-performing VLM models for various tasks, reducing the limitations in model selection and boosting system performance across a range of visual tasks. This shows that our method is not only highly effective in the present but also holds the potential for continued improvement as the model hub grows.

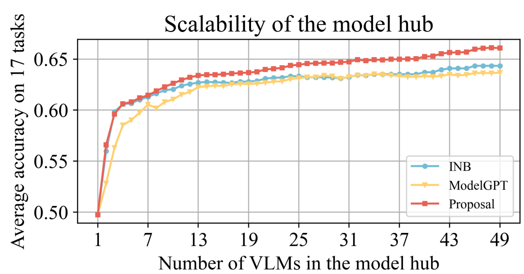

Figure 3: The average performance on 17 downstream tasks with the scaling of the model hub

6 Conclusion

In this paper, we explore how to select and reuse pre-trained VLMs for a specific downstream task. To the best of our knowledge, this problem has been rarely studied. To address this, we propose a novel paradigm called Model Label Learning (MLL) that assigns each VLM a label to describe its utility on representative visual concepts. The MLL paradigm contains three key modules: *model labeling*, *model selection*, and *model reuse*. The proposal is highly efficient, scalable, and convenient for both model developers and users. Moreover, we introduced a benchmark for evaluating pre-trained VLM selection and reuse methods that contain 49 pre-trained VLMs and 17 target datasets, with ground-truth ranking for each target task. Experiments demonstrate the proposal can achieve state-of-the-art model selection performance for VLMs and the ability to deal with downstream tasks could grow with the scale of the model hub, showing the potential of building large model hubs with advanced model selection mechanisms.

In future work, we will endeavor to develop a novel model hub based on the MLL paradigm presented in this paper, allowing valid VLM developers from all over the world to submit their models. When users work on visual classification tasks, they will be able to select and reuse models from the hub. The limitation of this paper is that the current implementation focuses solely on VLMs and visual classification tasks. We will further attempt to extend our paradigm to more model types that have significant architectural differences compared with VLMs, and more complex tasks.

REFERENCES

Krizhevsky Alex. Learning multiple layers of features from tiny images. 2009.

Lukas Bossard, Matthieu Guillaumin, and Luc Van Gool. Food-101–mining discriminative components with random forests. In *Proceedings of the 13th European Conference on Computer Vision*, pp. 446–461, 2014.

Gong Cheng, Junwei Han, and Xiaoqiang Lu. Remote sensing image scene classification: Benchmark and state of the art. *Proceedings of the IEEE*, 105(10):1865–1883, 2017.

Mircea Cimpoi, Subhransu Maji, Iasonas Kokkinos, Sammy Mohamed, and Andrea Vedaldi. Describing textures in the wild. In *Proceedings of the IEEE Conference on Computer Vision and Pattern Recognition*, pp. 3606–3613, 2014.

Adam Coates, Andrew Ng, and Honglak Lee. An analysis of single-layer networks in unsupervised feature learning. In *Proceedings of the 14th International Conference on Artificial Intelligence and Statistics*, pp. 215–223, 2011.

Jia Deng, Wei Dong, Richard Socher, Li-Jia Li, Kai Li, and Li Fei-Fei. ImageNet: A large-scale hierarchical image database. In *Proceedings of 2009 IEEE Conference on Computer Vision and Pattern Recognition*, pp. 248–255, 2009.

Alexey Dosovitskiy, Lucas Beyer, Alexander Kolesnikov, Dirk Weissenborn, Xiaohua Zhai, Thomas Unterthiner, Mostafa Dehghani, Matthias Minderer, Georg Heigold, Sylvain Gelly, Jakob Uszkoreit, and Neil Houlsby. An image is worth 16x16 words: Transformers for image recognition at scale. In *Proceedings of the 9th International Conference on Learning Representations*, 2021.

Alex Fang, Gabriel Ilharco, Mitchell Wortsman, Yuhao Wan, Vaishaal Shankar, Achal Dave, and Ludwig Schmidt. Data determines distributional robustness in Contrastive Language Image Pretraining (CLIP). In *Proceedings of the 39th International Conference on Machine Learning*, pp. 6216–6234, 2022.

Yuxin Fang, Wen Wang, Binhui Xie, Quan Sun, Ledell Wu, Xinggang Wang, Tiejun Huang, Xinlong Wang, and Yue Cao. EVA: Exploring the limits of masked visual representation learning at scale. In *Proceedings of the IEEE/CVF Conference on Computer Vision and Pattern Recognition*, pp. 19358–19369, 2023.

Ian J Goodfellow, Dumitru Erhan, Pierre Luc Carrier, Aaron Courville, Mehdi Mirza, Ben Hamner, Will Cukierski, Yichuan Tang, David Thaler, Dong-Hyun Lee, et al. Challenges in representation learning: A report on three machine learning contests. In *Proceedings of the 20th International Conference on Neural Information Processing*, pp. 117–124, 2013.

Lan-Zhe Guo, Zhi Zhou, Yu-Feng Li, and Zhi-Hua Zhou. Identifying useful learnwares for heterogeneous label spaces. In *Proceedings of the 40th International Conference on Machine Learning*, pp. 12122–12131, 2023.

Dan Hendrycks, Steven Basart, Norman Mu, Saurav Kadavath, Frank Wang, Evan Dorundo, Rahul Desai, Tyler Zhu, Samyak Parajuli, Mike Guo, et al. The many faces of robustness: A critical analysis of out-of-distribution generalization. In *Proceedings of the IEEE/CVF International Conference on Computer Vision*, pp. 8340–8349, 2021a.

Dan Hendrycks, Kevin Zhao, Steven Basart, Jacob Steinhardt, and Dawn Song. Natural adversarial examples. In *Proceedings of the IEEE/CVF Conference on Computer Vision and Pattern Recognition*, pp. 15262–15271, 2021b.

Gabriel Ilharco, Mitchell Wortsman, Ross Wightman, Cade Gordon, Nicholas Carlini, Rohan Taori, Achal Dave, Vaishaal Shankar, Hongseok Namkoong, John Miller, Hannaneh Hajishirzi, Ali Farhadi, and Ludwig Schmidt. OpenCLIP, 2021.

Chao Jia, Yinfei Yang, Ye Xia, Yi-Ting Chen, Zarana Parekh, Hieu Pham, Quoc Le, Yun-Hsuan Sung, Zhen Li, and Tom Duerig. Scaling up visual and vision-language representation learning with noisy text supervision. In *Proceedings of the 38th International Conference on Machine Learning*, pp. 4904–4916, 2021.

Justin Johnson, Bharath Hariharan, Laurens Van Der Maaten, Li Fei-Fei, C Lawrence Zitnick, and Ross Girshick. CLEVR: A diagnostic dataset for compositional language and elementary visual reasoning. In *Proceedings of the IEEE Conference on Computer Vision and Pattern Recognition*, pp. 2901–2910, 2017.

Jonathan Krause, Michael Stark, Jia Deng, and Li Fei-Fei. 3D object representations for fine-grained categorization. In *Proceedings of the IEEE International Conference on Computer Vision Workshops*, pp. 554–561, 2013.

Yann LeCun, Léon Bottou, Yoshua Bengio, and Patrick Haffner. Gradient-based learning applied to document recognition. *Proceedings of the IEEE*, 86(11):2278–2324, 1998.

Junnan Li, Dongxu Li, Caiming Xiong, and Steven Hoi. BLIP: Bootstrapping language-image pre-training for unified vision-language understanding and generation. In *Proceedings of the 39th International Conference on Machine Learning*, pp. 12888–12900, 2022.

Zhuang Liu, Hanzi Mao, Chao-Yuan Wu, Christoph Feichtenhofer, Trevor Darrell, and Saining Xie. A ConvNet for the 2020s. In *Proceedings of the IEEE/CVF Conference on Computer Vision and Pattern Recognition*, pp. 11976–11986, 2022.

Fanqing Meng, Wenqi Shao, Zhanglin Peng, Chonghe Jiang, Kaipeng Zhang, Yu Qiao, and Ping Luo. Foundation model is efficient multimodal multitask model selector. In *Advances in Neural Information Processing Systems*, pp. 33065–33094, 2023.

George A. Miller. WordNet: A lexical database for English. *Communications of the ACM*, 38(11): 39–41, 1995.

Cuong Nguyen, Tal Hassner, Matthias Seeger, and Cedric Archambeau. LEEP: A new measure to evaluate transferability of learned representations. In *Proceedings of the 37th International Conference on Machine Learning*, pp. 7294–7305, 2020.

Maria-Elena Nilsback and Andrew Zisserman. Automated flower classification over a large number of classes. In *Proceedings of 2008 6th Indian Conference on Computer Vision, Graphics & Image Processing*, pp. 722–729, 2008.

OpenAI. GPT-4 technical report. *CoRR*, abs/2303.08774, 2023.

Namyong Park, Ryan A Rossi, Nesreen Ahmed, and Christos Faloutsos. MetaGL: Evaluation-free selection of graph learning models via meta-learning. In *Proceedings of the 11th International Conference on Learning Representations*, 2023.

Omkar M Parkhi, Andrea Vedaldi, Andrew Zisserman, and CV Jawahar. Cats and dogs. In *Proceedings of 2012 IEEE Conference on Computer Vision and Pattern Recognition*, pp. 3498–3505, 2012.

Alec Radford, Jong Wook Kim, Chris Hallacy, Aditya Ramesh, Gabriel Goh, Sandhini Agarwal, Girish Sastry, Amanda Askell, Pamela Mishkin, Jack Clark, et al. Learning transferable visual models from natural language supervision. In *Proceedings of the 38th International Conference on Machine Learning*, pp. 8748–8763, 2021.

Benjamin Recht, Rebecca Roelofs, Ludwig Schmidt, and Vaishaal Shankar. Do ImageNet classifiers generalize to ImageNet? In *Proceedings of the 36th International conference on Machine Learning*, pp. 5389–5400, 2019.

Christoph Schuhmann, Romain Beaumont, Richard Vencu, Cade Gordon, Ross Wightman, Mehdi Cherti, Theo Coombes, Aarush Katta, Clayton Mullis, Mitchell Wortsman, et al. LAION-5B: An open large-scale dataset for training next generation image-text models. In *Advances in Neural Information Processing Systems*, pp. 25278–25294, 2022.

Khurram Soomro, Amir Roshan Zamir, and Mubarak Shah. UCF101: A dataset of 101 human actions classes from videos in the wild. *CoRR*, abs/1212.0402, 2012.

Krishna Srinivasan, Karthik Raman, Jiecao Chen, Michael Bendersky, and Marc Najork. WIT: Wikipedia-based image text dataset for multimodal multilingual machine learning. In *Proceedings of the 44th International ACM SIGIR Conference on Research and Development in Information Retrieval*, pp. 2443–2449, 2021.

Johannes Stallkamp, Marc Schlipsing, Jan Salmen, and Christian Igel. Man vs. computer: Benchmarking machine learning algorithms for traffic sign recognition. *Neural Networks*, 32:323–332, 2012.

Peng Tan, Zhi-Hao Tan, Yuan Jiang, and Zhi-Hua Zhou. Handling learnwares developed from heterogeneous feature spaces without auxiliary data. In *Proceedings of the 32nd International Joint Conference on Artificial Intelligence*, pp. 4235–4243, 2023.

Zhi-Hao Tan, Jian-Dong Liu, Xiao-Dong Bi, Peng Tan, Qin-Cheng Zheng, Hai-Tian Liu, Yi Xie, Xiao-Chuan Zou, Yang Yu, and Zhi-Hua Zhou. Beimingwu: A learnware dock system. In *Proceedings of the 30th ACM SIGKDD Conference on Knowledge Discovery and Data Mining*, pp. 5773–5782, 2024.

Anh T Tran, Cuong V Nguyen, and Tal Hassner. Transferability and hardness of supervised classification tasks. In *Proceedings of the IEEE/CVF International Conference on Computer Vision*, pp. 1395–1405, 2019.

Bastiaan S Veeling, Jasper Linmans, Jim Winkens, Taco Cohen, and Max Welling. Rotation equivariant CNNs for digital pathology. In *Proceedings of the 21st International Conference on Medical Image Computing and Computer Assisted Intervention*, pp. 210–218, 2018.

Haohan Wang, Songwei Ge, Zachary Lipton, and Eric P Xing. Learning robust global representations by penalizing local predictive power. In *Advances in Neural Information Processing Systems*, 2019.

Thomas Wolf, Lysandre Debut, Victor Sanh, Julien Chaumond, Clement Delangue, Anthony Moi, Pierric Cistac, Tim Rault, Rémi Louf, Morgan Funtowicz, et al. Transformers: State-of-the-art natural language processing. In *Proceedings of 2020 Conference on Empirical Methods in Natural Language Processing*, pp. 38–45, 2020.

Xi-Zhu Wu, Wenkai Xu, Song Liu, and Zhi-Hua Zhou. Model reuse with reduced kernel mean embedding specification. *IEEE Transactions on Knowledge and Data Engineering*, 35(1):699–710, 2021.

Kaichao You, Yong Liu, Jianmin Wang, and Mingsheng Long. LogME: Practical assessment of pre-trained models for transfer learning. In *Proceedings of the 38th International Conference on Machine Learning*, pp. 12133–12143, 2021.

Jiahui Yu, Zirui Wang, Vijay Vasudevan, Legg Yeung, Mojtaba Seyedhosseini, and Yonghui Wu. CoCa: Contrastive captioners are image-text foundation models. *Transactions on Machine Learning Research*, 2022.

Xiaohua Zhai, Joan Puigcerver, Alexander Kolesnikov, Pierre Ruyssen, Carlos Riquelme, Mario Lucic, Josip Djolonga, Andre Susano Pinto, Maxim Neumann, Alexey Dosovitskiy, et al. A large-scale study of representation learning with the visual task adaptation benchmark. *CoRR*, abs/1910.04867, 2019.

Yi-Kai Zhang, Ting-Ji Huang, Yao-Xiang Ding, De-Chuan Zhan, and Han-Jia Ye. Model spider: Learning to rank pre-trained models efficiently. *Advances in Neural Information Processing Systems*, pp. 13692–13719, 2024.

Zhi-Hua Zhou and Zhi-Hao Tan. Learnware: Small models do big. *CoRR*, abs/2210.03647, 2022.

Orr Zohar, Shih-Cheng Huang, Kuan-Chieh Wang, and Serena Yeung. LOVM: Language-only vision model selection. In *Advances in Neural Information Processing Systems*, pp. 33120–33132, 2023.

A DETAILS OF BENCHMARK

In this section, we provide detailed insights into our benchmark utilized for evaluating VLM selection and reuse methods. Table 2 presents general information on the model hub, including model architecture, pre-trained datasets, parameters, FLOPs, and accuracy on ImageNet. Table 3 outlines the datasets used in the benchmark, highlighting the type of domain and task for each dataset. This breakdown is essential for understanding the context and effectiveness of the models assessed in our study.

Table 2: Details on model hub used in the benchmark, which contain the model architecture, pre-trained datasets, parameters, FLOPs, and Accuracy on ImageNet

ID	Model Architecture	Pretrained Dataset	Params (M)	FLOPs (B)	ImageNet Acc.
1	RN50	openai	102.01	18.18	0.5982
2	RN50	cc12m	102.01	18.18	0.3591
3	RN101	openai	119.69	25.5	0.6228
4	RN101	yfcc15m	119.69	25.5	0.3407
5	RN101-quickgelu	openai	119.69	25.5	0.6228
6	RN101-quickgelu	yfcc15m	119.69	25.5	0.3487
7	RN50x4	openai	178.3	51.82	0.6627
8	RN50x64	openai	623.26	552.65	0.7391
9	ViT-B-32	openai	151.28	14.78	0.6332
10	ViT-B-32	laion2b_e16	151.28	14.78	0.6565
11	ViT-B-32	datacomp_xl_s13b_b90k	151.28	14.78	0.6917
12	ViT-B-32	commonpool_m_clip_s128m_b4k	151.28	14.78	0.2725
13	ViT-B-32-256	datacomp_s34b_b86k	151.29	17.46	0.7281
14	ViT-B-32-quickgelu	laion400m_e31	151.28	14.78	0.6294
15	ViT-B-32-quickgelu	metaclip_fullcc	151.28	14.78	0.6766
16	ViT-B-16	openai	149.62	41.09	0.6834
17	ViT-B-16	laion2b_s34b_b88k	149.62	41.09	0.7023
18	ViT-B-16	datacomp_l_s1b_b8k	149.62	41.09	0.6310
19	ViT-B-16	commonpool_l_laion_s1b_b8k	149.62	41.09	0.5526
20	ViT-B-16	dfn2b	149.62	41.09	0.7624
21	ViT-B-16-quickgelu	metaclip_fullcc	149.62	41.09	0.7212
22	ViT-B-16-plus-240	laion400m_e31	208.38	64.03	0.6904
23	ViT-L-14	openai	427.62	175.33	0.7554
24	ViT-L-14	laion400m_e31	427.62	175.33	0.7271
25	ViT-L-14	datacomp_xl_s13b_b90k	427.62	175.33	0.7921
26	ViT-L-14	commonpool_xl_clip_s13b_b90k	427.62	175.33	0.7637
27	ViT-L-14-quickgelu	metaclip_fullcc	427.62	175.33	0.7917
28	ViT-L-14-quickgelu	dfn2b	427.62	175.33	0.8141
29	ViT-L-14-336	openai	427.94	395.22	0.7656
30	ViT-H-14	laion2b_s32b_b79k	986.11	381.68	0.7796
31	ViT-H-14-quickgelu	metaclip_fullcc	986.11	381.68	0.8051
32	ViT-H-14-378-quickgelu	dfn5b	986.71	1054.05	0.8437
33	ViT-g-14	laion2b_s12b_b42k	1366.68	581.15	0.7663
34	ViT-bigG-14	laion2b_s39b_b160k	2539.57	1065.36	0.8009
35	roberta-ViT-B-32	laion2b_s12b_b32k	212.72	105.87	0.6171
36	xlm-roberta-base-ViT-B-32	laion5b_s13b_b90k	366.12	105.87	0.6236
37	convnext_base_w	laion2b_s13b_b82k	179.39	49.38	0.7078
38	convnext_base_w_320	laion_aesthetic_s13b_b82k	179.39	71.94	0.7167
39	convnext_large_d	laion2b_s26b_b102k_augreg	351.77	107.5	0.7591
40	convnext_large_d_320	laion2b_s29b_b131k_ft	351.77	157.98	0.7660
41	convnext_xxlarge	laion2b_s34b_b82k_augreg_soup	1200.58	443.03	0.7947
42	coca_ViT-B-32	laion2b_s13b_b90k	253.56	33.34	0.6331
43	coca_ViT-L-14	laion2b_s13b_b90k	638.45	214.52	0.7561
44	EVA01-g-14	laion400m_s11b_b41k	1136.44	547.36	0.7852
45	EVA02-B-16	merged2b_s8b_b131k	149.69	41.09	0.7472
46	EVA02-L-14-336	merged2b_s6b_b61k	428.08	395.16	0.8039
47	EVA02-E-14	laion2b_s4b_b115k	4704.59	2311.42	0.8196
48	nllb-clip-base	v1	501.89	369.6	0.2432
49	nllb-clip-base-siglip	v1	507.47	472.91	0.3909

Table 3: Details on the datasets used in the benchmark, which contain the type of domain and task.

Dataset	Domain	Task
ImageNet (Deng et al., 2009)	natural picture	image classification
ImageNet-V2 (Recht et al., 2019)	natural picture	image classification
ImageNet-Sketch (Wang et al., 2019)	Sketch picture	image classification
ImageNet-A (Hendrycks et al., 2021b)	natural picture	image classification
ImageNet-R (Hendrycks et al., 2021a)	15 domain picture (e.g., art, cartoon)	image classification
CIFAR100 (Alex, 2009)	natural picture	image classification
Country211 (Radford et al., 2021)	natural picture	geo-localization
CLEVR-D (Johnson et al., 2017)	natural picture	object distance estimation
DTD (Cimpoi et al., 2014)	texture picture	image classification
DMLab (Zhai et al., 2019)	natural picture	object distance estimation
Flowers102 (Nilsback & Zisserman, 2008)	flower picture	image classification
FER2013 (Goodfellow et al., 2013)	facial picture	facial expression classification
Food101 (Bossard et al., 2014)	food picture	image classification
GTSRB (Stallkamp et al., 2012)	traffic picture	image classification
MNIST (LeCun et al., 1998)	digit picture	image classification
OxfordIIITPet (Parkhi et al., 2012)	pet photograph	image classification
PCam (Veeling et al., 2018)	medical picture	image classification
Rendered SST2 (Radford et al., 2021)	text picture	optical character recognition
RESISC45 (Cheng et al., 2017)	satellite picture	land cover classification
StanfordCars (Krause et al., 2013)	car picture	image classification
STL10 (Coates et al., 2011)	natural picture	image classification
UCF101 (Soomro et al., 2012)	video frame	action recognition